EUROPEAN ORGANIZATION FOR NUCLEAR RESEARCH

CERN-EP/99-127
September 20, 1999

Search for Charginos and Neutralinos in e^+e^- collisions at $\sqrt{s} = 189$ GeV

The L3 collaboration

Abstract

We report the result of a search for charginos and neutralinos, in e^+e^- collisions at 189 GeV centre-of-mass energy at LEP. No evidence for such particles is found in a data sample of 176 pb^{-1}. Improved upper limits for these particles are set on the production cross sections. New exclusion contours in the parameter space of the Minimal Supersymmetric Standard Model are derived, as well as new lower limits on the masses of these supersymmetric particles. Under the assumptions of common gaugino and scalar masses at the GUT scale, we set an absolute lower limit on the mass of the lightest neutralino of 32.5 GeV and on the mass of the lightest chargino of 67.7 GeV.

Submitted to *Phys. Lett. B*

1 Introduction

One of the main goals of the LEP experiments is to search for new particles predicted by theories beyond the Standard Model. In this letter we report on searches for unstable charginos and neutralinos. These particles are predicted by supersymmetric theories (SUSY) [1]. In SUSY theories with minimal particle content (MSSM) [2], in addition to the ordinary particles, there is a supersymmetric spectrum of particles with spins which differ by one half with respect to their Standard Model partners.

Charginos ($\tilde{\chi}^{\pm}_{1,2}$), the supersymmetric partners of $\mathrm{W}^{\pm}$ and $\mathrm{H}^{\pm}$, are pair produced via s-channel γ/Z exchange. The production cross section can be reduced by an order of magnitude when the t-channel scalar neutrino ($\tilde{\nu}$) exchange is important. Neutralinos, the supersymmetric partners of Z, γ, and neutral Higgs bosons, are pair produced $\mathrm{e^+e^-} \rightarrow \tilde{\chi}^0_i\tilde{\chi}^0_j$ $(i,j = 1,\ldots,4$; ordered by their masses) via s-channel Z exchange and their production cross section can be enhanced by t-channel exchange of a scalar electron ($\tilde{\mathrm{e}}^{\pm}$).

Short-lived supersymmetric particles are expected in R-parity conserving SUSY models. The R-parity is a quantum number which distinguishes ordinary particles from supersymmetric particles. If R-parity is conserved, supersymmetric particles are pair-produced and the lightest supersymmetric particle, assumed to be the lightest neutralino, $\tilde{\chi}^0_1$, is stable. The neutralino is weakly-interacting and escapes detection. In this letter we assume R-parity conservation, which implies that the decay chain of supersymmetric particles always contain, besides standard particles, two invisible neutralinos causing the missing energy signature.

When the masses of the scalar leptons and the charged Higgs bosons ($\mathrm{H}^{\pm}$) are very large, the $\tilde{\chi}^{\pm}_1$ decays via W^*: $\tilde{\chi}^{\pm}_1 \rightarrow \tilde{\chi}^0_1\mathrm{W}^* \rightarrow \tilde{\chi}^0_1 f\bar{f}'$. If the $\tilde{\ell}^{\pm}$ and $\tilde{\nu}$ masses are comparable to M_{W} the chargino also decays via virtual scalar lepton or scalar neutrino and the leptonic branching fraction is enhanced. Finally for $\tilde{\ell}^{\pm}$ and $\tilde{\nu}$ lighter than the chargino, the decay modes $\tilde{\chi}^{\pm}_1 \rightarrow \tilde{\ell}^{\pm}\nu$ or $\tilde{\chi}^{\pm}_1 \rightarrow \tilde{\nu}\ell^{\pm}$ become dominant. When the masses of the neutral SUSY Higgs bosons (h^0, A^0) and of the scalar leptons are very large, the heavier neutralinos ($\tilde{\chi}^0_j$, $j \geq 2$) decay via Z^*: $\tilde{\chi}^0_j \rightarrow \tilde{\chi}^0_k\mathrm{Z}^* \rightarrow \tilde{\chi}^0_k f\bar{f}$ with $k < j$. For a chargino lighter than neutralinos, the latter decay via W^* such as $\tilde{\chi}^0_j \rightarrow \tilde{\chi}^{\pm}_1 f\bar{f}'$. If the scalar lepton masses are comparable to the Z mass, the neutralino decays also via a virtual scalar lepton, enhancing the leptonic branching fraction. Finally, for $\tilde{\nu}$ and $\tilde{\ell}^{\pm}$ lighter than neutralinos the two-body decays $\tilde{\chi}^0_j \rightarrow \tilde{\ell}^{\pm}\ell^{\mp}$ or $\tilde{\chi}^0_j \rightarrow \tilde{\nu}\nu$ ($\mathrm{j} \geq 2$) become dominant. The radiative decays $\tilde{\chi}^0_j \rightarrow \tilde{\chi}^0_k\gamma$ are also possible via higher-order diagrams.

Previous results on chargino and neutralino searches have been reported by L3 [3–5] and other LEP experiments [6]. In this letter, new limits are presented on chargino and neutralino production cross sections. These experimental results are interpreted in the framework of the constrained MSSM. Within these models lower limits on the masses of supersymmetric particles are derived. For these limits present experimental results are combined with those obtained previously by L3 at the Z peak [7] and at energies up to $\sqrt{s} = 183$ GeV [3–5, 8].

2 Data Sample and Simulation

We present the analysis of data collected by the L3 detector [9] in 1998, corresponding to an integrated luminosity of 176.3 pb^{-1} at an average centre-of-mass energy of 188.6 GeV, denoted hereafter as $\sqrt{s} = 189$ GeV.

Standard Model reactions are simulated with the following Monte Carlo generators: `PYTHIA` [10] for $\mathrm{e^+e^-} \rightarrow \mathrm{q\bar{q}}$, $\mathrm{e^+e^-} \rightarrow \mathrm{Z\,e^+e^-}$ and $\mathrm{e^+e^-} \rightarrow \gamma/\mathrm{Z}\,\gamma/\mathrm{Z}$; `EXCALIBUR` [11] for $\mathrm{e^+e^-} \rightarrow \mathrm{W^{\pm}\,e^{\mp}}\nu$;

KORALZ [12] for $e^+e^- \to \mu^+\mu^-$ and $e^+e^- \to \tau^+\tau^-$; BHWIDE [13] for $e^+e^- \to e^+e^-$; KORALW [14] for $e^+e^- \to W^+W^-$; two-photon interaction processes have been simulated using DIAG36 [15] ($e^+e^- \to e^+e^-\ell^+\ell^-$) and PHOJET [16] ($e^+e^- \to e^+e^-$ hadrons), requiring at least 3 GeV for the invariant mass of the two-photon system. The number of simulated events for each background process is equivalent to more than 100 times the statistics of the collected data sample except for two-photon interactions for which it is more than two times the data statistics.

Signal events are generated with the Monte Carlo program SUSYGEN [17], for masses of SUSY particles ($M_{\rm SUSY}$) ranging from 45 GeV up to the kinematic limit and for ΔM values ($\Delta M = M_{\rm SUSY} - M_{\tilde{\chi}^0_1}$) between 3 GeV and $M_{\rm SUSY} - 1$ GeV. The explicit two-body decay branching ratios for charginos $\tilde{\chi}^\pm_1 \to \tilde{\nu}\ell^\pm, \tilde{\ell}^\pm\nu$ or $\tilde{\chi}^0_{2,3,4} \to \tilde{\nu}\nu, \tilde{\ell}\ell$ have been estimated with SUSYGEN.

The detector response is simulated using the GEANT package [18]. It takes into account effects of energy loss, multiple scattering and showering in the detector materials and in the beam pipe. Hadronic interactions are simulated with the GHEISHA program [19]. Time dependent inefficiencies of the different subdetectors are also taken into account in the simulation procedure.

3 Analysis Procedure

3.1 Signal topologies and optimisation procedure

Besides the main characteristic of missing transverse momentum, supersymmetric particle signals can be further specified according to the number of leptons or the multiplicity of hadronic jets in the final state. As mentioned in the introduction, chargino pair production gives final states similar to WW production. For neutralinos, we distinguish two classes of detectable processes: $e^+e^- \to \tilde{\chi}^0_1\tilde{\chi}^0_2$ and $e^+e^- \to \tilde{\chi}^0_2\tilde{\chi}^0_2$. For these signals, final states are given by the Z branching ratios. Both for charginos and neutralinos, the event energy is directly related to ΔM ($\Delta M = M_{\rm SUSY} - M_{\tilde{\chi}^0_1}$).

We devise five types of selection criteria oriented to all decays of charginos, as follows: at least two acoplanar leptons (e,μ); hadrons and at least one isolated lepton; at least two acoplanar taus; hadrons and at least one isolated tau; purely hadronic final states with high multiplicity. $\tilde{\chi}^0_2\tilde{\chi}^0_2$ production gives rise to final states very similar to those of chargino pair production, even if with very different branching ratios. Hence, chargino selections based on these five topologies are also effective to select $\tilde{\chi}^0_2\tilde{\chi}^0_2$ events.

The two-acoplanar-jets final state on the other hand deserves a dedicated selection since it accounts for 70% of the decays in $\tilde{\chi}^0_1\tilde{\chi}^0_2$ events, and 28% in $\tilde{\chi}^0_2\tilde{\chi}^0_2$ events.

The signal topologies and the associated background sources depend strongly on ΔM. Therefore the selections are optimised separately for four different ΔM ranges: the very low ΔM range at $3-5$ GeV, the low ΔM range at $10-30$ GeV, the medium ΔM range at $40-70$ GeV and the high ΔM range at $80-94$ GeV. In the low and very low ΔM ranges, the expected topologies for the signal are characterised by a low multiplicity and a low visible energy, and the background is dominated by two-photon interactions. For medium and high ΔM charginos, the signal signatures are very similar to those of W-pair production; in particular for $\Delta M > 80$ GeV on-shell Ws are produced.

The cut values of each selection are *a priori* optimised using Monte Carlo signal and background events. The optimisation procedure varies all cuts simultaneously to maximise the signal efficiency and the background rejection. In fact, the average limit (κ^{-1}) is minimised for an infinite number of tries, assuming only background contributions. This is expressed mathematically by the following formula:

$$\kappa = \epsilon / \Sigma_{n=0}^{\infty} k(b)_n P(b,n) \tag{1}$$

where $k(b)_n$ is the 95% confidence level Bayesian upper limit, $P(b,n)$ is the Poisson distribution for n events with an expected background of b events, and ϵ is the signal efficiency.

3.2 Event selection

Lepton and photon identification, and isolation criteria in hadronic events are unchanged compared to our previous analysis [4]. The Durham algorithm [20] is used for the clustering of hadronic jets.

Events are first selected by requiring at least 3 GeV of visible energy and 3 GeV of transverse momentum. Beam-gas events are rejected by requiring the visible energy in a cone of 30° around the beam pipe (E_{30^0}) to be less than 90% of the total and the missing momentum vector to be at least 10° away from the beam pipe. Tagged two-photon interactions are rejected by requiring the sum of the energies measured in the lead-scintillator ring calorimeter and in the luminosity monitors [9] to be less than 10 GeV. These two detectors cover the polar angle range $1.5^\circ < \theta < 9^\circ$ on both sides of the interaction point.

3.2.1 Leptonic final states

For the pure leptonic final states, dedicated selections have been optimised for the charginos, where the two leptons may have a different flavour. Those selections are very similar to the scalar lepton selections which are described in Reference [21]. At the end, a combination of all the leptonic selections, providing the optimal sensitivity (κ of Formula 1), is done for the chargino and the neutralino leptonic decays.

3.2.2 Lepton plus hadrons final states

We select events with at least one isolated electron, muon or tau for which the energy, not associated to the lepton, in a cone of 30° half-opening angle around its direction is less than 2 GeV. The following quantities are defined: the energy depositions ($E_{25}^{\perp}$ and E_{25}) within $\pm 25^\circ$ around the missing energy direction in the R–ϕ plane or in space, respectively. We apply cuts on the number of tracks in the hadronic system ($N_{tk} - N_{lep}$) and the number of calorimetric clusters (N_{cl}). Furthermore, cuts are applied on the missing energy direction isolation (θ_{miss} and $E_{25}^{\perp}$), the total transverse momentum ($p_{\perp}$), the energy of the isolated lepton (E_{lep}), the recoil mass (M_{rec}), as well as on the acoplanarity angle between the jet and the lepton. A cut is applied on the visible energy (E_{vis}) and E_{TTJL} which is defined as the absolute value of the projection of the total momentum of the jet and the lepton onto the direction perpendicular to the lepton-jet thrust computed in the R-ϕ plane. A cut on the invariant mass of the hadronic system (M_{had}) removes most of the WW background.

The cut values at $\sqrt{s} = 189$ GeV, are shown in Table 1 for the different ΔM ranges.

3.2.3 Purely hadronic final states

The list of cuts used at $\sqrt{s} = 189$ GeV is reported in Table 2 for the different ΔM ranges. Again, we apply cuts on N_{cl}, N_{tk}, $p_{\perp}$, E_{vis}, acollinearity and acoplanarity as well as on the missing energy polar angle (θ_{miss}) and isolation ($E_{25}^{\perp}$, E_{25}). The absolute value of the total momentum of the event along the beam line normalised to the visible energy ($p_{\parallel}$), the recoil mass (M_{rec}) and the visible mass (M_{vis}) are also used in the selections.

In all the selections, but the very low ΔM, a cut on the width of the two jets is applied. We define $y_{\perp}$ as the ratio between the scalar sum of the particle momenta transverse to the jet direction and the jet energy. We require $y_{\perp}$ to be large in order to select four-jet-like events. In the low ΔM range a cut on the ratio $E_{TTJ}/p_{\perp}$ is applied. E_{TTJ} is equivalent to E_{TTJL} using the momenta and the directions of the two jets.

4 Results

The results at $\sqrt{s}$ = 189 GeV, for the eighteen chargino selections and the four neutralino selections are shown in Table 3. The results for the very low and low ΔM selections are shown together. A good agreement between the expected background from Standard Model processes and the selected data is observed.

The eighteen chargino selections find 147 candidates in the data when expecting 148 events from the Standard Model processes. In the low and very low ΔM regions 72 events are selected, 11 events in the medium ΔM region and 67 events in the high ΔM region. In the four neutralino selections 50 candidates are found whereas 48.1 events are expected from the Standard Model processes, most of those events are selected by the low ΔM selections.

Each selection is parametrised as a function of a single parameter, ξ, in the following manner: given a lower edge, X^i_{loose}, and an upper edge, X^i_{tight}, for the cut on the variable i, the parameter ξ is equal to 0 when this cut is at the lower edge (many background events satisfy the selection) and 100 when it is at the upper edge (no or few background events pass the selection). All cuts ($i = 1, ..., N$) are related to the parameter ξ as follows:

$$X^i_{cut} = X^i_{loose} + (X^i_{tight} - X^i_{loose}) \times \frac{\xi}{100}.$$

The parameter ξ is scanned around the optimal value (ξ=50) to check the agreement between data and Monte Carlo at different background rejection stages. As illustrated in Figure 1 for the lepton and hadrons final state in chargino decays and the pure hadronic final state in the neutralino decays, the data and Monte Carlo simulations are in good agreement for all the ΔM selections. The vertical arrows show the ξ value corresponding to the optimised cuts.

For intermediate ΔM values different from those chosen for optimisation we choose the combination of selections providing the highest sensitivity [4]. In this combination procedure, we take into account the overlap among the selections within the data and Monte Carlo samples.

Typical selection efficiencies, as well as the number of background events expected for a chargino mass of 94 GeV for the purely leptonic final state (LL) or for the $\mathrm{W}^*\tilde{\chi}^0_1$ decay mode, are displayed in Table 4. In the latter case, a maximum efficiency of 47% is reached for a background contamination of 7.5 events for ΔM = 30 GeV. In the low ΔM region the efficiency decreases due to the large contamination of two-photon interactions and due to the lower trigger acceptance. For large ΔM it decreases because of the WW background.

The selection efficiencies, as well as the number of background events expected for a sum of neutralino masses $M_{\tilde{\chi}^0_1} + M_{\tilde{\chi}^0_2}$ = 188 GeV for the pure leptonic decays and for the $\mathrm{Z}^*\tilde{\chi}^0_1$ decay mode are displayed in Table 5. Compared to the chargino selection, the efficiencies are lower due to the invisible decays of the Z^*.

Systematic errors on the signal efficiencies are evaluated as in Reference 3, and they are typically 5% relative, dominated by Monte Carlo statistics. Systematic errors on the background prediction are in general 2% except for two-photon processes for which they can be as large as 10%. These errors are taken into account following a procedure similar to that explained in Reference 22.

5 Model independent upper limits on production cross sections

No excess of events is observed and we set upper limits on the chargino and neutralino production cross sections in the framework of the MSSM. Exclusion limits at 95% C.L. are derived taking into account background contributions.

To derive the upper limits on production cross sections and for interpretations in the MSSM we combine the $\sqrt{s} = 189$ GeV data sample with those collected by L3 at lower centre-of-mass energies [3–5].

The contours of upper limits on the luminosity weighted average production cross section for the process $\mathrm{e^+e^-} \rightarrow \tilde{\chi}_1^\pm \tilde{\chi}_1^\mp$ are shown in Figure 2 assuming $\tilde{\chi}_1^\pm \rightarrow \mathrm{W}^* \tilde{\chi}_1^0$ for the chargino decay with standard W branching fractions, and for purely leptonic W decays. In most of the kinematically accessible region, cross sections larger than 0.2 pb are excluded for both scenarios.

Similarly, luminosity weighted average cross section limits for associated neutralino production $\mathrm{e^+e^-} \rightarrow \tilde{\chi}_1^0 \tilde{\chi}_2^0$ are derived as shown in Figure 3 assuming $\tilde{\chi}_2^0 \rightarrow \mathrm{Z}^* \tilde{\chi}_1^0$, with standard Z branching fractions and for purely leptonic Z decays. In most of the kinematically accessible region, cross sections larger than 0.3 pb are excluded for both scenarios.

6 Interpretation in the MSSM

In the MSSM, with Grand Unification assumptions [23], the masses and couplings of the SUSY particles as well as their production cross sections, are entirely described [2] once five parameters are fixed: $\tan\beta$, the ratio of the vacuum expectation values of the two Higgs doublets, $M \equiv M_2$, the gaugino mass parameter, μ, the higgsino mixing parameter, m_0, the common mass for scalar fermions at the GUT scale, and A, the trilinear coupling in the Higgs sector. The following MSSM parameter space is investigated:

$$\begin{array}{rclcrcl} 0.7 \leq & \tan\beta & \leq 60, & & 0 \leq & M_2 & \leq 2000 \text{ GeV}, \\ -2000 \text{ GeV} \leq & \mu & \leq 2000 \text{ GeV}, & & 0 \leq & m_0 & \leq 500 \text{ GeV}. \end{array}$$

To derive the absolute limits on the masses of the lightest neutralino and of the lightest chargino, a scan in the MSSM parameter space is performed in steps of 0.2 GeV for M_2, 1.0 GeV for μ and 0.5 GeV for m_0.

Mass eigenstates of scalar quarks and leptons are in general a mixture of the weak eigenstates $\tilde{\mathrm{f}}_R$ and $\tilde{\mathrm{f}}_L$. The mixing between these two states is proportional to the mass of the partner fermion. Hence the mixing can be sizable only for particles of the third generation. The mixing is governed by the parameters A, μ and $\tan\beta$.

All the limits on the cross sections previously shown, combined with the results obtained at lower centre-of-mass energies and with the results of scalar lepton searches obtained at $\sqrt{s} = 189$ GeV [21], can be translated into exclusion regions in the MSSM parameter space.

To derive limits in the MSSM, we optimise the global selection for any different point in the parameter space. This is obtained, choosing every time the combination of selections providing the highest sensitivity, given the production cross sections and the decay branching fractions which are calculated with the generator `SUSYGEN`. In general, all limits are evaluated neglecting the mixing in the scalar tau sector.

This mixing is instead considered in the mSUGRA framework and masses and decay branching fractions are recalculated by using the generator `ISAJET` [24]. In this framework a scan on the A parameter between –500 GeV and 500 GeV with a 10 GeV step is performed and the validity of the mass limits on chargino and neutralino is checked.

6.1 Limits on chargino and neutralino masses

In the MSSM, while the cross sections and decay branching fractions of the charginos and neutralinos depend on the masses of the scalar leptons, their masses depend only on M_2, μ and $\tan\beta$. The exclusions in the high m_0 range are derived from chargino and neutralino searches, while for low m_0 the searches for scalar leptons [21], and for photons and missing energy final states [25], also contribute. We also take into account all chargino and neutralino cascade decays:

- $\tilde{\chi}^{\pm}_1 \rightarrow \tilde{\chi}^0_2\,\mathrm{W}^*$: we observe a slight decrease of the efficiency relative to $\tilde{\chi}^{\pm}_1 \rightarrow \tilde{\chi}^0_1\,\mathrm{W}^*$. The decrease depends on the mass of $\tilde{\chi}^0_2$, which is varied between the $\tilde{\chi}^{\pm}_1$ and $\tilde{\chi}^0_1$ masses. The lowest efficiency is then used for cascade decays.

- $\tilde{\chi}^0_{3,4} \rightarrow \tilde{\chi}^0_2\,\mathrm{Z}^*$: the efficiency is found to be larger than the efficiency obtained for the $\tilde{\chi}^0_{3,4} \rightarrow \tilde{\chi}^0_1\,\mathrm{Z}^*$ channel, especially in the high ΔM region. The efficiencies obtained in the latter channel are used.

- $\tilde{\chi}^0_{3,4} \rightarrow \tilde{\nu}\nu$: when the $\tilde{\nu}$ becomes detectable through its cascade decays into $\tilde{\chi}^0_2$ or $\tilde{\chi}^{\pm}_1$. This is especially relevant in the mixed region ($\mu \sim -M_2$) for the low $\tan\beta$ values.

Depending on the neutralino-chargino field content, one distinguishes the following cases for the determination of lower limits on the neutralino and chargino masses:

- Higgsino-like $\tilde{\chi}^0_2$ and $\tilde{\chi}^{\pm}_1$ ($M_2 \gg |\mu|$): in this case, the production cross sections do not depend on the scalar lepton masses, ΔM is low and decreases with increasing M_2. Consequently, the limits on the masses of the next-to-lightest neutralino and the lightest chargino decrease with M_2 as depicted in Figure 4. For $\tan\beta = \sqrt{2}$ and M_2 less than 500 GeV, $M_{\tilde{\chi}^0_2} \leq 101$ GeV and $M_{\tilde{\chi}^{\pm}_1} \leq 93$ GeV are excluded.

- Gaugino-like $\tilde{\chi}^{\pm}_1$ ($|\mu| \gg M_2$): the chargino cross section depends strongly on the scalar neutrino mass. For 50 GeV $\leq M_{\tilde{\nu}} \leq$ 80 GeV the cross section is reduced by one order of magnitude compared to what is expected for $M_{\tilde{\nu}} \geq$ 500 GeV. When the two body decay $\tilde{\chi}^{\pm}_1 \rightarrow \ell^{\pm}\,\tilde{\nu}$ is dominant, the relevant ΔM becomes $\Delta M = M_{\tilde{\chi}^{\pm}_1} - M_{\tilde{\nu}}$. If the $\tilde{\nu}$ is mass degenerate with the $\tilde{\chi}^{\pm}_1$ the acceptance is substantially reduced. However, when this occurs scalar leptons are light and the experimental sensitivity is recovered with these channels.

The mass limit of the lightest chargino is shown in Figure 5 as a function of $\tan\beta$ for all the different chargino field contents. At large $\tan\beta$ values, the lower mass limit of the lightest chargino is obtained when the lightest chargino and the $\tilde{\nu}$ are mass degenerate (gaugino region).

At low $\tan\beta$ values the lower mass limit on the lightest chargino is obtained when the lightest chargino and the $\tilde{\chi}_1^0$ (LSP) are mass degenerate (higgsino region). Finally, for $M_2 < 2$ TeV, for $\tan\beta \leq 60$ and for any m_0 values, the lower mass limit of the lightest chargino is:

$$M_{\tilde{\chi}_1^\pm} \geq 67.7 \text{ GeV}.$$

The scalar tau can be much lighter than the scalar electron and muon. This mass splitting occurs in particular for large $\tan\beta$ and A values. When this happens, chargino and next-to-lightest neutralino decays are affected. Therefore, detection efficiencies are estimated for chargino and next-to-lightest neutralino decays with 100% branching ratio into $\tilde{\tau}_1\nu$ and $\tilde{\tau}_1^\pm\tau^\mp$, respectively. In particular, when the $\tilde{\tau}_1$ and the LSP are mass degenerate the efficiencies decrease substantially. However, the experimental sensitivity can be partially recovered taking into account also the process $\mathrm{e}^+\mathrm{e}^- \rightarrow \tilde{\nu}\tilde{\nu}$, where the $\tilde{\nu}$ is visible through its cascade decays. In particular, within the mSUGRA framework the limit on the chargino mass holds for any value of the mixing if $\tan\beta < 20$. For higher $\tan\beta$ values this limit can be decreased at most by 10 GeV.

Indirect limits on the mass of the lightest neutralino are also derived as a function of m_0 and as a function of $\tan\beta$. In the low m_0 region (≤ 65 GeV) the mass limit on the LSP comes mainly from the scalar lepton searches. For large m_0 values (≥ 200 GeV), only the chargino and neutralino searches contribute. At low $\tan\beta$ the processes $\mathrm{e}^+\mathrm{e}^- \rightarrow \tilde{\chi}_2^0\tilde{\chi}_{3,4}^0$ contribute significantly and they are taken into account. The lower mass limit is found at $\tan\beta = 1$, $\mu = -70$ GeV and $m_0 = 500$ GeV, as shown in Figure 6. For these values of the parameters, the chargino mass is at the kinematic limit and the mass difference between the chargino and the LSP is maximal.

For intermediate m_0 values (65 GeV $\leq m_0 \leq$ 95 GeV) the production cross section for charginos is minimal and the $\tilde{\nu}$ is light enough to allow the following decay modes: $\tilde{\chi}_{2,3,4}^0 \rightarrow \tilde{\nu}\nu$ and $\tilde{\chi}_1^\pm \rightarrow \tilde{\nu}\ell^\pm$. This is the region where the exclusion is due to the interplay of many different searches. The limit on the lightest neutralino as a function of m_0, and for two extreme values of $\tan\beta$, is shown in Figure 7. For low $\tan\beta$ values ($\leq \sqrt{2}$), the minimum is found for $\mu \sim -70$ GeV and large m_0 values. Better limits are obtained for intermediate m_0 values, where the neutralino production cross sections are large and the two body decays of the $\tilde{\chi}_{3,4}^0$ into $\tilde{\nu}\nu$ are visible through the cascade decays of the $\tilde{\nu}$. For larger $\tan\beta$ values, the minimum is found in the gaugino region (-2000 GeV $< \mu < -200$ GeV) and for 70 GeV $\leq m_0 \leq$ 80 GeV. In this region of the parameter space, the $\tilde{\nu}$ and the chargino are mass degenerate, the heavier neutralinos decay invisibly and the experimental sensitivity is entirely due to the scalar lepton searches.

Finally in Figure 8, the mass limit on the lightest neutralino as a function of $\tan\beta$ for any m_0 value is shown. For $\tan\beta \geq 0.7$, the lower mass limit of the lightest neutralino is

$$M_{\tilde{\chi}_1^0} \geq 32.5 \text{ GeV}.$$

The mass limit on the lightest neutralino is very little affected by the mixing in the scalar tau sector. The limit, within the mSUGRA framework, holds for any value of the mixing if $\tan\beta < 20$ and it can be reduced at most by 1.5 GeV for higher $\tan\beta$ values. Nevertheless, the absolute mass limit for the lightest neutralino does not change since the lowest value is still found at $\tan\beta = 1$.

We also derive an absolute limit on M_2. This is shown as a function of $\tan\beta$ for any m_0 and μ as depicted in Figure 9. Values of M_2 lower than 54.8 GeV are now excluded at 95% C.L.

Acknowledgments

We express our gratitude to the CERN accelerator divisions for the excellent performance of the LEP machine. We also acknowledge and appreciate the effort of the engineers, technicians and support staff who have participated in the construction and maintenance of this experiment.

References

[1] Y.A. Golfand and E.P. Likhtman, Sov. Phys. JETP **13** (1971) 323;
D.V. Volkhov and V.P. Akulov, Phys. Lett. **B 46** (1973) 109;
J. Wess and B. Zumino, Nucl. Phys. **B 70** (1974) 39;
P. Fayet and S. Ferrara, Phys. Rep. **C 32** (1977) 249;
A. Salam and J. Strathdee, Fortschr. Phys. **26** (1978) 57.

[2] H. P. Nilles, Phys. Rep. **110** (1984) 1;
H. E. Haber and G. L. Kane, Phys. Rep. **117** (1985) 75;
R. Barbieri, Nuovo Cimento **11** No. 4 (1988) 1.

[3] L3 Collab., M. Acciarri *et al.*, Phys. Lett. **B 377** (1996) 289.

[4] L3 Collab., M. Acciarri *et al.*, Eur. Phys. Journal **C 4** (1998) 207.

[5] L3 Collab., M. Acciarri *et al.*, contributed paper n. 493 to *ICHEP98*, Vancouver, July 1998.

[6] ALEPH Collab., R. Barate *et al.*, CERN-EP-99-014 (1999);
DELPHI Collab., P. Abreu *et al.*, Phys. Lett. **B 446** (1999) 75;
OPAL Collab., G. Abbiendi *et al.*, Eur. Phys. Journal **C 8** (1999) 255.

[7] L3 Collab., O. Adriani *et al.*, Phys. Rep. **236** (1993) 1;
L3 Collab., M. Acciarri *et al.*, Phys. Lett. **B 350** (1995) 109.

[8] L3 Collab., M. Acciarri *et al.*, Phys. Lett. **B 456** (1999) 283.

[9] L3 Collab., B. Adeva *et al.*, Nucl. Instr. and Meth. **A 289** (1990) 35;
M. Chemarin *et al.*, Nucl. Instr. and Meth. **A 349** (1994) 345;
M. Acciarri *et al.*, Nucl. Instr. and Meth. **A 351** (1994) 300;
G. Basti *et al.*, Nucl. Instr. and Meth. **A 374** (1996) 293;
I.C. Brock *et al.*, Nucl. Instr. and Meth. **A 381** (1996) 236;
A. Adam *et al.*, Nucl. Instr. and Meth. **A 383** (1996) 342.

[10] T. Sjöstrand, "PYTHIA 5.7 and JETSET 7.4 Physics and Manual",
CERN–TH/7112/93 (1993), revised August 1995;
T. Sjöstrand, Comp. Phys. Comm. **82** (1994) 74.

[11] `EXCALIBUR` version 1.11 is used.
F.A. Berends, R. Kleiss and R. Pittau, Nucl. Phys. **B 424** (1994) 308; Nucl. Phys. **B 426** (1994) 344; Nucl. Phys. (Proc. Suppl.) **B 37** (1994) 163; Phys. Lett. **B 335** (1994) 490; Comp. Phys. Comm. **83** (1994) 141.

[12] KORALZ version 4.02 is used.
S. Jadach, B.F.L. Ward and Z. Wąs, Comp. Phys. Comm. **79** (1994) 503.

[13] BHWIDE version 1.01 is used.
S. Jadach *et al.*, Phys. Lett. **B 390** (1997) 298.

[14] KORALW version 1.33 is used.
M. Skrzypek *et al.*, Comp. Phys. Comm. **94** (1996) 216;
M. Skrzypek *et al.*, Phys. Lett. **B 372** (1996) 289.

[15] F.A. Berends, P.H. Daverfeldt and R. Kleiss, Nucl. Phys. **B 253** (1985) 441.

[16] PHOJET version 1.10 is used.
R. Engel, Z. Phys. **C 66** (1995) 203;
R. Engel and J. Ranft, Phys. Rev. **D 54** (1996) 4244.

[17] SUSYGEN version 2.2 is used.
S. Katsanevas and P. Morawitz, Comp. Phys. Comm. **112** (1998) 227.

[18] The L3 detector simulation is based on GEANT Version 3.15.
See R. Brun *et al.*, "GEANT 3", CERN DD/EE/84-1 (Revised), September 1987.

[19] H. Fesefeldt, RWTH Aachen Preprint PITHA 85/02 (1985).

[20] S. Catani *et al.*, Phys. Lett. **B 269** (1991) 432;
S. Bethke *et al.*, Nucl. Phys. **B 370** (1992) 310.

[21] L3 Collab., M. Acciarri *et al.*, *Search for Scalar leptons in* e^+e^- *collisions at* $\sqrt{s}$*=189 GeV*, contributed paper n. 7-46 to *EPS-HEP99*, Tampere, July 1999, and also submitted to Phys. Lett.

[22] R.D. Cousins and V.L. Highland, Nucl. Inst. Meth. **A 320** (1992) 331.

[23] See for instance:
L. Ibanez, Phys. Lett. **B 118** (1982) 73;
R. Barbieri, S. Farrara and C. Savoy, Phys. Lett. **B 119** (1982) 343.

[24] ISAJET version 7.44 is used.
H. Baer *et al.*, BNL-HET-98-39, (1998), hep-ph/9810440.

[25] L3 Collab., M. Acciarri *et al.*, Phys. Lett. **B 444** (1998) 503.

The L3 Collaboration:

M.Acciarri,[26] P.Achard,[19] O.Adriani,[16] M.Aguilar-Benitez,[25] J.Alcaraz,[25] G.Alemanni,[22] J.Allaby,[17] A.Aloisio,[28] M.G.Alviggi,[28] G.Ambrosi,[19] H.Anderhub,[47] V.P.Andreev,[6,36] T.Angelescu,[12] F.Anselmo,[9] A.Arefiev,[27] T.Azemoon,[3] T.Aziz,[10] P.Bagnaia,[35] L.Baksay,[42] A.Balandras,[4] R.C.Ball,[3] S.Banerjee,[10] Sw.Banerjee,[10] A.Barczyk,[47,45] R.Barillère,[17] L.Barone,[35] P.Bartalini,[22] M.Basile,[9] R.Battiston,[32] A.Bay,[22] F.Becattini,[16] U.Becker,[14] F.Behner,[47] L.Bellucci,[16] J.Berdugo,[25] P.Berges,[14] B.Bertucci,[32] B.L.Betev,[47] S.Bhattacharya,[10] M.Biasini,[32] A.Biland,[47] J.J.Blaising,[4] S.C.Blyth,[33] G.J.Bobbink,[2] A.Böhm,[1] L.Boldizsar,[13] B.Borgia,[35] D.Bourilkov,[47] M.Bourquin,[19] S.Braccini,[19] J.G.Branson,[38] V.Brigljevic,[47] F.Brochu,[4] A.Buffini,[16] A.Buijs,[43] J.D.Burger,[14] W.J.Burger,[32] J.Busenitz,[42] A.Button,[3] X.D.Cai,[14] M.Campanelli,[47] M.Capell,[14] G.Cara Romeo,[9] G.Carlino,[28] A.M.Cartacci,[16] J.Casaus,[25] G.Castellini,[16] F.Cavallari,[35] N.Cavallo,[28] C.Cecchi,[19] M.Cerrada,[25] F.Cesaroni,[23] M.Chamizo,[19] Y.H.Chang,[49] U.K.Chaturvedi,[18] M.Chemarin,[24] A.Chen,[49] G.Chen,[7] G.M.Chen,[7] H.F.Chen,[20] H.S.Chen,[7] X.Chereau,[4] G.Chiefari,[28] L.Cifarelli,[37] F.Cindolo,[9] C.Civinini,[16] I.Clare,[14] R.Clare,[14] G.Coignet,[4] A.P.Colijn,[2] N.Colino,[25] S.Costantini,[8] F.Cotorobai,[12] B.Cozzoni,[9] B.de la Cruz,[25] A.Csilling,[13] S.Cucciarelli,[32] T.S.Dai,[14] J.A.van Dalen,[30] R.D'Alessandro,[16] R.de Asmundis,[28] P.Déglon,[19] A.Degré,[4] K.Deiters,[45] D.della Volpe,[28] P.Denes,[34] F.DeNotaristefani,[35] A.De Salvo,[47] M.Diemoz,[35] D.van Dierendonck,[2] F.Di Lodovico,[47] C.Dionisi,[35] M.Dittmar,[47] A.Dominguez,[38] A.Doria,[28] M.T.Dova,[18,♯] D.Duchesneau,[4] D.Dufournaud,[4] P.Duinker,[2] I.Duran,[39] H.El Mamouni,[24] A.Engler,[33] F.J.Eppling,[14] F.C.Erné,[2] P.Extermann,[19] M.Fabre,[45] R.Faccini,[35] M.A.Falagan,[25] S.Falciano,[35,17] A.Favara,[17] J.Fay,[24] O.Fedin,[36] M.Felcini,[47] T.Ferguson,[33] F.Ferroni,[35] H.Fesefeldt,[1] E.Fiandrini,[32] J.H.Field,[19] F.Filthaut,[17] P.H.Fisher,[14] I.Fisk,[38] G.Forconi,[14] L.Fredj,[19] K.Freudenreich,[47] C.Furetta,[26] Yu.Galaktionov,[27,14] S.N.Ganguli,[10] P.Garcia-Abia,[5] M.Gataullin,[31] S.S.Gau,[11] S.Gentile,[35,17] N.Gheordanescu,[12] S.Giagu,[35] Z.F.Gong,[20] G.Grenier,[24] O.Grimm,[47] M.W.Gruenewald,[8] M.Guida,[37] R.van Gulik,[2] V.K.Gupta,[34] A.Gurtu,[10] L.J.Gutay,[44] D.Haas,[5] A.Hasan,[29] D.Hatzifotiadou,[9] T.Hebbeker,[8] A.Hervé,[17] P.Hidas,[13] J.Hirschfelder,[33] H.Hofer,[47] G. Holzner,[47] H.Hoorani,[33] S.R.Hou,[49] I.Iashvili,[46] B.N.Jin,[7] L.W.Jones,[3] P.de Jong,[2] I.Josa-Mutuberría,[25] R.A.Khan,[18] D.Kamrad,[46] M.Kaur,[18,◇] M.N.Kienzle-Focacci,[19] D.Kim,[35] D.H.Kim,[41] J.K.Kim,[41] S.C.Kim,[41] J.Kirkby,[17] D.Kiss,[13] W.Kittel,[30] A.Klimentov,[14,27] A.C.König,[30] A.Kopp,[46] I.Korolko,[27] V.Koutsenko,[14,27] M.Kräber,[47] R.W.Kraemer,[33] W.Krenz,[1] A.Kunin,[14,27] P.Ladron de Guevara,[25] I.Laktineh,[24] G.Landi,[16] K.Lassila-Perini,[47] P.Laurikainen,[21] A.Lavorato,[37] M.Lebeau,[17] A.Lebedev,[14] P.Lebrun,[24] P.Lecomte,[47] P.Lecoq,[17] P.Le Coultre,[47] H.J.Lee,[8] J.M.Le Goff,[17] R.Leiste,[46] E.Leonardi,[35] P.Levtchenko,[36] C.Li,[20] C.H.Lin,[49] W.T.Lin,[49] F.L.Linde,[2] L.Lista,[28] Z.A.Liu,[7] W.Lohmann,[46] E.Longo,[35] Y.S.Lu,[7] K.Lübelsmeyer,[1] C.Luci,[17,35] D.Luckey,[14] L.Lugnier,[24] L.Luminari,[35] W.Lustermann,[47] W.G.Ma,[20] M.Maity,[10] L.Malgeri,[17] A.Malinin,[27,17] C.Maña,[25] D.Mangeol,[30] P.Marchesini,[47] G.Marian,[15] J.P.Martin,[24] F.Marzano,[35] G.G.G.Massaro,[2] K.Mazumdar,[10] R.R.McNeil,[6] S.Mele,[17] L.Merola,[28] M.Meschini,[16] W.J.Metzger,[30] M.von der Mey,[1] A.Mihul,[12] H.Milcent,[17] G.Mirabelli,[35] J.Mnich,[17] G.B.Mohanty,[10] P.Molnar,[8] B.Monteleoni,[16,†] T.Moulik,[10] G.S.Muanza,[24] F.Muheim,[19] A.J.M.Muijs,[2] M.Musy,[35] M.Napolitano,[28] F.Nessi-Tedaldi,[47] H.Newman,[31] T.Niessen,[1] A.Nisati,[35] H.Nowak,[46] Y.D.Oh,[41] G.Organtini,[35] R.Ostonen,[21] C.Palomares,[25] D.Pandoulas,[1] S.Paoletti,[35,17] P.Paolucci,[28] R.Paramatti,[35] H.K.Park,[33] I.H.Park,[41] G.Pascale,[35] G.Passaleva,[17] S.Patricelli,[28] T.Paul,[11] M.Pauluzzi,[32] C.Paus,[17] F.Pauss,[47] D.Peach,[17] M.Pedace,[35] S.Pensotti,[26] D.Perret-Gallix,[4] B.Petersen,[30] D.Piccolo,[28] F.Pierella,[9] M.Pieri,[16] P.A.Piroué,[34] E.Pistolesi,[26] V.Plyaskin,[27] M.Pohl,[47] V.Pojidaev,[27,16] H.Postema,[14] J.Pothier,[17] N.Produit,[19] D.O.Prokofiev,[44] D.Prokofiev,[36] J.Quartieri,[37] G.Rahal-Callot,[47,17] M.A.Rahaman,[10] P.Raics,[15] N.Raja,[10] R.Ramelli,[47] P.G.Rancoita,[26] G.Raven,[38] P.Razis,[29]D.Ren,[47] M.Rescigno,[35] S.Reucroft,[11] T.van Rhee,[43] S.Riemann,[46] K.Riles,[3] A.Robohm,[47] J.Rodin,[42] B.P.Roe,[3] L.Romero,[25] A.Rosca,[8] S.Rosier-Lees,[4] J.A.Rubio,[17] D.Ruschmeier,[8] H.Rykaczewski,[47] S.Saremi,[6] S.Sarkar,[35] J.Salicio,[17] E.Sanchez,[17] M.P.Sanders,[30] M.E.Sarakinos,[21] C.Schäfer,[1] V.Schegelsky,[36] S.Schmidt-Kaerst,[1] D.Schmitz,[1] H.Schopper,[48] D.J.Schotanus,[30] G.Schwering,[1] C.Sciacca,[28] D.Sciarrino,[19] A.Seganti,[9] L.Servoli,[32] S.Shevchenko,[31] N.Shivarov,[40] V.Shoutko,[27] E.Shumilov,[27] A.Shvorob,[31] T.Siedenburg,[1] D.Son,[41] B.Smith,[33] P.Spillantini,[16] M.Steuer,[14] D.P.Stickland,[34] A.Stone,[6] H.Stone,[34,†] B.Stoyanov,[40] A.Straessner,[1] K.Sudhakar,[10] G.Sultanov,[18] L.Z.Sun,[20] H.Suter,[47] J.D.Swain,[18] Z.Szillasi,[42,¶] T.Sztaricskai,[42,¶] X.W.Tang,[7] L.Tauscher,[5] L.Taylor,[11] C.Timmermans,[30] Samuel C.C.Ting,[14] S.M.Ting,[14] S.C.Tonwar,[10] J.Tóth,[13] C.Tully,[34] K.L.Tung,[7]Y.Uchida,[14] J.Ulbricht,[47] E.Valente,[35] G.Vesztergombi,[13] I.Vetlitsky,[27] D.Vicinanza,[37] G.Viertel,[47] S.Villa,[11] M.Vivargent,[4] S.Vlachos,[5] I.Vodopianov,[36] H.Vogel,[33] H.Vogt,[46] I.Vorobiev,[27] A.A.Vorobyov,[36] A.Vorvolakos,[29] M.Wadhwa,[5] W.Wallraff,[1] M.Wang,[14] X.L.Wang,[20] Z.M.Wang,[20] A.Weber,[1] M.Weber,[1] P.Wienemann,[1] H.Wilkens,[30] S.X.Wu,[14] S.Wynhoff,[1] L.Xia,[31] Z.Z.Xu,[20] B.Z.Yang,[20] C.G.Yang,[7] H.J.Yang,[7] M.Yang,[7] J.B.Ye,[20] S.C.Yeh,[50] An.Zalite,[36] Yu.Zalite,[36] Z.P.Zhang,[20] G.Y.Zhu,[7] R.Y.Zhu,[31] A.Zichichi,[9,17,18] F.Ziegler,[46] G.Zilizi,[42,¶] M.Zöller.[1]

1 I. Physikalisches Institut, RWTH, D-52056 Aachen, FRG[§]
III. Physikalisches Institut, RWTH, D-52056 Aachen, FRG[§]
2 National Institute for High Energy Physics, NIKHEF, and University of Amsterdam, NL-1009 DB Amsterdam, The Netherlands
3 University of Michigan, Ann Arbor, MI 48109, USA
4 Laboratoire d'Annecy-le-Vieux de Physique des Particules, LAPP,IN2P3-CNRS, BP 110, F-74941 Annecy-le-Vieux CEDEX, France
5 Institute of Physics, University of Basel, CH-4056 Basel, Switzerland
6 Louisiana State University, Baton Rouge, LA 70803, USA
7 Institute of High Energy Physics, IHEP, 100039 Beijing, China[△]
8 Humboldt University, D-10099 Berlin, FRG[§]
9 University of Bologna and INFN-Sezione di Bologna, I-40126 Bologna, Italy
10 Tata Institute of Fundamental Research, Bombay 400 005, India
11 Northeastern University, Boston, MA 02115, USA
12 Institute of Atomic Physics and University of Bucharest, R-76900 Bucharest, Romania
13 Central Research Institute for Physics of the Hungarian Academy of Sciences, H-1525 Budapest 114, Hungary[‡]
14 Massachusetts Institute of Technology, Cambridge, MA 02139, USA
15 Lajos Kossuth University-ATOMKI, H-4010 Debrecen, Hungary[¶]
16 INFN Sezione di Firenze and University of Florence, I-50125 Florence, Italy
17 European Laboratory for Particle Physics, CERN, CH-1211 Geneva 23, Switzerland
18 World Laboratory, FBLJA Project, CH-1211 Geneva 23, Switzerland
19 University of Geneva, CH-1211 Geneva 4, Switzerland
20 Chinese University of Science and Technology, USTC, Hefei, Anhui 230 029, China[△]
21 SEFT, Research Institute for High Energy Physics, P.O. Box 9, SF-00014 Helsinki, Finland
22 University of Lausanne, CH-1015 Lausanne, Switzerland
23 INFN-Sezione di Lecce and Universitá Degli Studi di Lecce, I-73100 Lecce, Italy
24 Institut de Physique Nucléaire de Lyon, IN2P3-CNRS,Université Claude Bernard, F-69622 Villeurbanne, France
25 Centro de Investigaciones Energéticas, Medioambientales y Tecnologícas, CIEMAT, E-28040 Madrid, Spain♭
26 INFN-Sezione di Milano, I-20133 Milan, Italy
27 Institute of Theoretical and Experimental Physics, ITEP, Moscow, Russia
28 INFN-Sezione di Napoli and University of Naples, I-80125 Naples, Italy
29 Department of Natural Sciences, University of Cyprus, Nicosia, Cyprus
30 University of Nijmegen and NIKHEF, NL-6525 ED Nijmegen, The Netherlands
31 California Institute of Technology, Pasadena, CA 91125, USA
32 INFN-Sezione di Perugia and Universitá Degli Studi di Perugia, I-06100 Perugia, Italy
33 Carnegie Mellon University, Pittsburgh, PA 15213, USA
34 Princeton University, Princeton, NJ 08544, USA
35 INFN-Sezione di Roma and University of Rome, "La Sapienza", I-00185 Rome, Italy
36 Nuclear Physics Institute, St. Petersburg, Russia
37 University and INFN, Salerno, I-84100 Salerno, Italy
38 University of California, San Diego, CA 92093, USA
39 Dept. de Fisica de Particulas Elementales, Univ. de Santiago, E-15706 Santiago de Compostela, Spain
40 Bulgarian Academy of Sciences, Central Lab. of Mechatronics and Instrumentation, BU-1113 Sofia, Bulgaria
41 Center for High Energy Physics, Adv. Inst. of Sciences and Technology, 305-701 Taejon, Republic of Korea
42 University of Alabama, Tuscaloosa, AL 35486, USA
43 Utrecht University and NIKHEF, NL-3584 CB Utrecht, The Netherlands
44 Purdue University, West Lafayette, IN 47907, USA
45 Paul Scherrer Institut, PSI, CH-5232 Villigen, Switzerland
46 DESY, D-15738 Zeuthen, FRG
47 Eidgenössische Technische Hochschule, ETH Zürich, CH-8093 Zürich, Switzerland
48 University of Hamburg, D-22761 Hamburg, FRG
49 National Central University, Chung-Li, Taiwan, China
50 Department of Physics, National Tsing Hua University, Taiwan, China
§ Supported by the German Bundesministerium für Bildung, Wissenschaft, Forschung und Technologie
‡ Supported by the Hungarian OTKA fund under contract numbers T019181, F023259 and T024011.
¶ Also supported by the Hungarian OTKA fund under contract numbers T22238 and T026178.
♭ Supported also by the Comisión Interministerial de Ciencia y Tecnología.
♯ Also supported by CONICET and Universidad Nacional de La Plata, CC 67, 1900 La Plata, Argentina.
◊ Also supported by Panjab University, Chandigarh-160014, India.
△ Supported by the National Natural Science Foundation of China.
† Deceased.

Electron/Muon plus hadrons selections				
	Very Low ΔM	Low ΔM	Medium ΔM	Large ΔM
No. of isolated leptons $\geq$	1	1	1	1
$N_{tk} - N_{lep} \geq$	2	4	5	4
$N_{cl} \geq$	6	10	10	10
$\sin(\theta_{miss}) \geq$	0.74	0.38	0.23	0.28
$E_{25}^{\perp}$ (GeV) $\leq$	0.52	–	–	11.6
$p_{\perp}$ (GeV) $\geq$	3.24	5.62	8.65	9.84
E_{lep} (GeV) $\geq$	1.51	2.59	6.17	25.9
E_{lep} (GeV) $\leq$	9.12	27.5	31.2	43.8
E_{TTJL} (GeV) $\geq$	1.27	0.95	1.44	–
M_{had} (GeV) $\leq$	5.0	28.2	39.1	89.0
M_{rec} (GeV) $\geq$	144	130	107	57.0
E_{vis} (GeV) $\geq$	4.02	8.90	31.5	65.3
E_{vis} (GeV) $\leq$	11.0	59.1	93.6	118

Table 1: Values of the cuts for the lepton plus hadrons selections; they are determined with the optimisation procedure described in Section 3.1.

Chargino Hadronic selections				
	Very Low ΔM	Low ΔM	Medium ΔM	Large ΔM
$N_{cl} \geq$	14	14	14	14
$N_{tk} \geq$	5	5	5	5
$p_{\perp}$ (GeV) $\geq$	3.72	10.0	11.5	11.4
$p_{\perp}/E_{vis} \geq$	–	0.20	0.15	0.10
E_{vis} (GeV) $\leq$	12.0	68.0	76.0	149
Acollinearity (rad) $\leq$	2.00	–	–	3.02
Acoplanarity (rad) $\leq$	2.18	2.89	2.92	3.11
$\sin(\theta_{miss}) \geq$	0.56	0.46	0.20	0.61
$E_{25}^{\perp}$ (GeV) $\leq$	0.21	5.80	5.80	3.25
E_{25} (GeV) $\leq$	–	–	–	2.53
$p_{\parallel}/E_{vis} \leq$	–	0.53	0.95	0.55
E_{lep}^{max} (GeV) $\leq$	9.12	27.5	31.2	43.8
M_{vis} (GeV) $\geq$	2.85	9.3	35.4	–
M_{rec} (GeV) $\geq$	–	124	67.2	–
$E_{vis}/\sqrt{s} \geq$	–	–	–	0.60
$E_{30^0}/E_{vis} \leq$	–	0.22	0.40	0.65
$E_{TTJ}/p_{\perp} \geq$	0.24	–	0.24	–
$y_{\perp} \geq$	–	0.28	0.28	0.40

Table 2: Values of the cuts for the purely hadronic selections which are determined with the optimisation procedure described in Section 3.1.

	Low ΔM		Medium ΔM		High ΔM		Combined	
	N_{data}	N_{exp}	N_{data}	N_{exp}	N_{data}	N_{exp}	N_{data}	N_{exp}
$\tilde{\chi}^{\pm}$	72	66.9	11	10.9	67	76.7	147	148.
$\tilde{\chi}^0_2$	43	39.3	6	7.78	3	2.45	50	48.1

Table 3: Results for charginos and neutralinos: N_{data} is the number of observed events and N_{exp} is the number of expected events from Standard Model processes for the total integrated luminosity collected at $\sqrt{s} = 189$ GeV.

	LL		$\tilde{\chi}^0_1\,\mathrm{W}^*$	
ΔM (GeV)	ϵ (%)	N_{exp}	ϵ (%)	N_{exp}
3	1.6	20.3	1.9	39.4
5	6.5	20.3	16.8	76.8
10	19.2	27.7	8.5	2.9
20	25.0	7.3	38.2	10.4
30	30.0	7.3	46.6	7.5
40	28.9	7.3	44.2	4.9
50	26.9	7.3	25.3	4.9
60	21.6	7.3	16.6	4.9
75	34.5	34.6	20.8	55.5
90	31.8	34.6	7.8	55.5

Table 4: Optimised chargino efficiencies (ϵ) for the purely leptonic (LL) and for the $\tilde{\chi}^0_1\,\mathrm{W}^*$ decay mode. N_{exp} is the number of events expected from Standard Model processes. Results are given as a function of ΔM for $M_{\tilde{\chi}^{\pm}_1} = 94$ GeV at $\sqrt{s} = 189$ GeV.

	LL		$\tilde{\chi}^0_1\,\mathrm{Z}^*$	
ΔM (GeV)	ϵ (%)	N_{exp}	ϵ (%)	N_{exp}
6	9.1	9.5	3.5	35.9
10	10.9	10.2	10.9	35.9
20	27.3	4.2	9.2	3.4
40	30.8	2.8	25.9	3.4
60	34.1	19.2	35.2	7.7
80	35.5	19.2	35.2	7.7
100	29.3	21.4	20.7	7.7
140	17.7	25.5	9.4	2.4
180	10.5	25.5	8.7	2.4

Table 5: Optimised neutralino efficiencies (ϵ) for the purely leptonic (LL) final states and for the $\tilde{\chi}^0_1\,\mathrm{Z}^*$ decay mode. Results are given as a function of ΔM for $M_{\tilde{\chi}^0_2} + M_{\tilde{\chi}^0_1} = 188$ GeV at $\sqrt{s} = 189$ GeV.

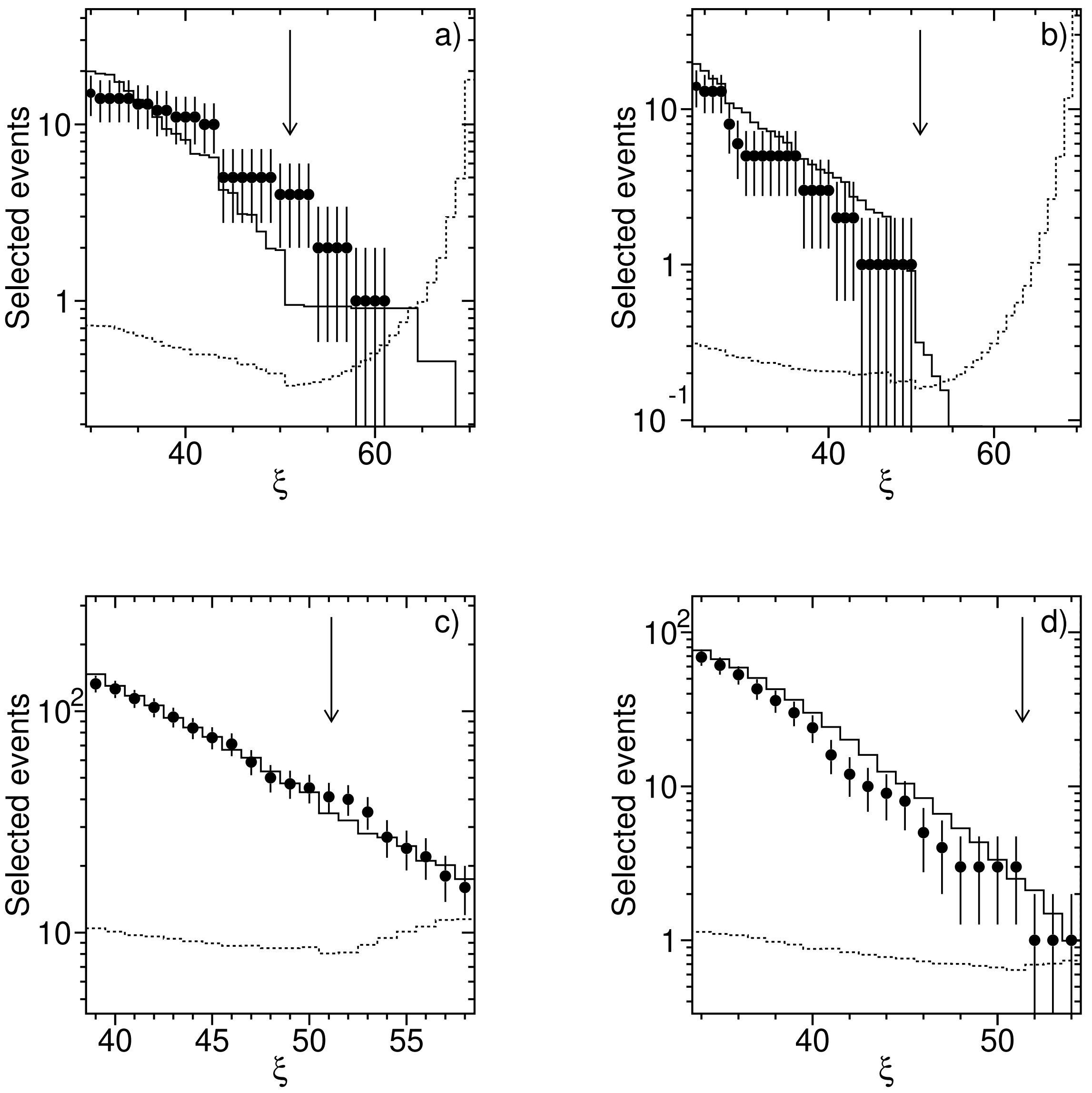

Figure 1: Number of events selected in data (points), in Monte Carlo simulation of standard processes (solid line) and signal sensitivity (dashed line) as a function of selection cuts with increasing background rejection power. The vertical arrows show the ξ value corresponding to the optimised cuts. The distributions are shown for the chargino lepton-jets low ΔM a), the chargino lepton-jets medium ΔM b), the neutralino jet-jet very low ΔM c) and the neutralino jet-jet high ΔM d) selections, respectively

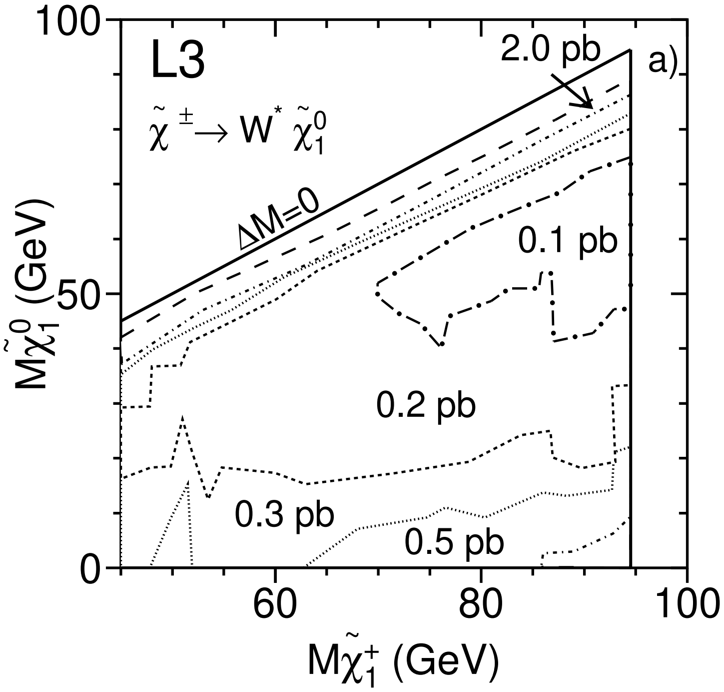

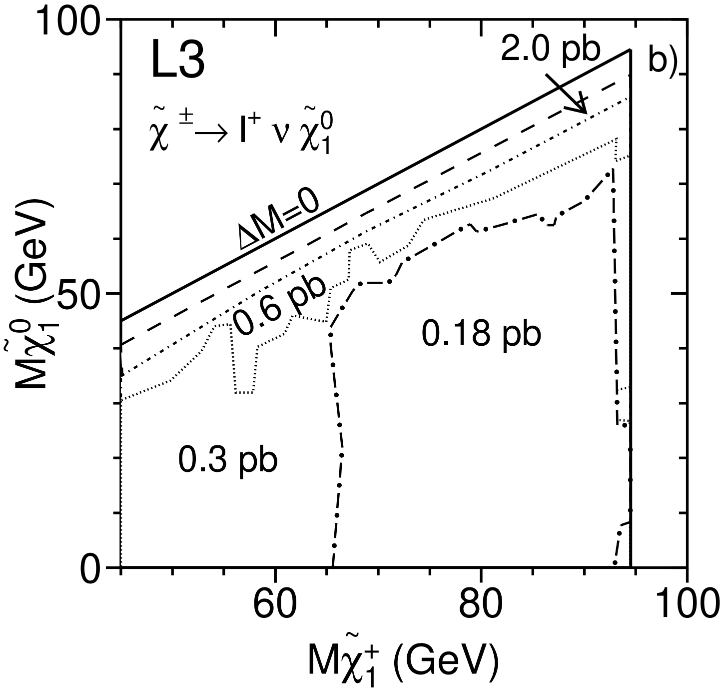

Figure 2: Upper limits on the $e^+e^- \rightarrow \tilde{\chi}_1^+\tilde{\chi}_1^-$ production cross section up to $\sqrt{s} = 189$ GeV in the $M_{\tilde{\chi}_1^0} - M_{\tilde{\chi}_1^\pm}$ plane. Exclusion limits are obtained assuming standard W branching ratios in the chargino decay a) or purely leptonic W decays b), $\tilde{\chi}_1^\pm \rightarrow \tilde{\chi}_1^0 \ell^\pm \nu$ ($\ell =$e, μ, τ).

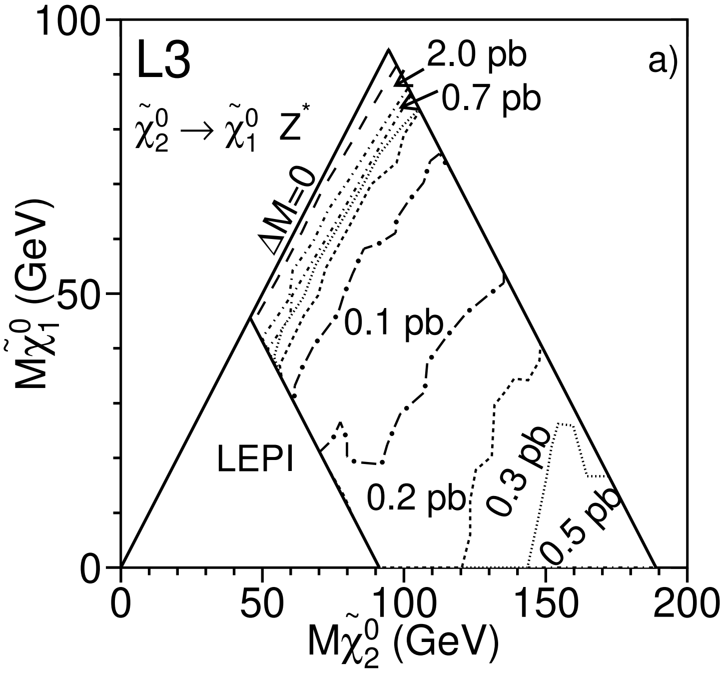

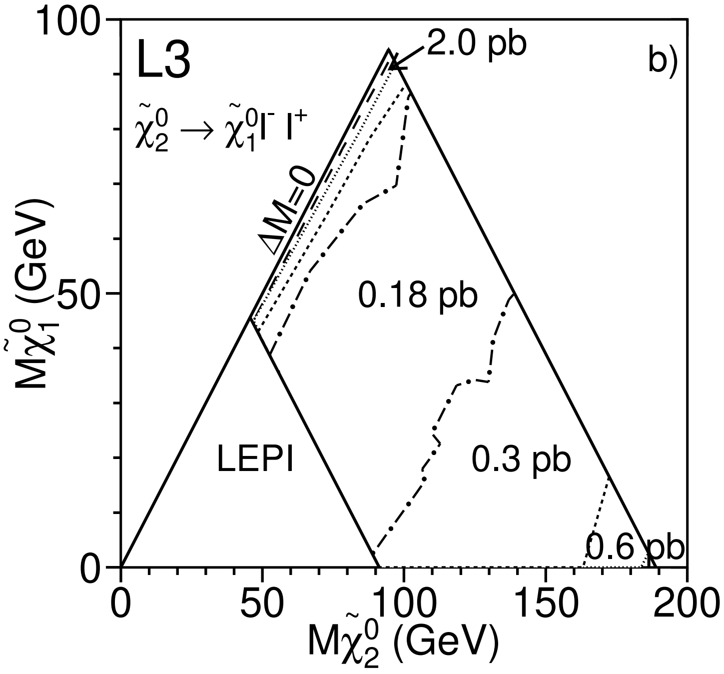

Figure 3: Upper limits on the $e^+e^- \to \tilde{\chi}^0_1\tilde{\chi}^0_2$ production cross section up to $\sqrt{s} = 189$ GeV in the $M_{\tilde{\chi}^0_1} - M_{\tilde{\chi}^0_2}$ plane. Exclusion limits are obtained assuming standard Z branching ratios in the next-to-lightest neutralino decay $\tilde{\chi}^0_2 \to Z^*\tilde{\chi}^0_1$ a) or assuming purely leptonic Z decays b), $\tilde{\chi}^0_2 \to \tilde{\chi}^0_1\ell^+\ell^-$ ($\ell =$e, μ, τ).

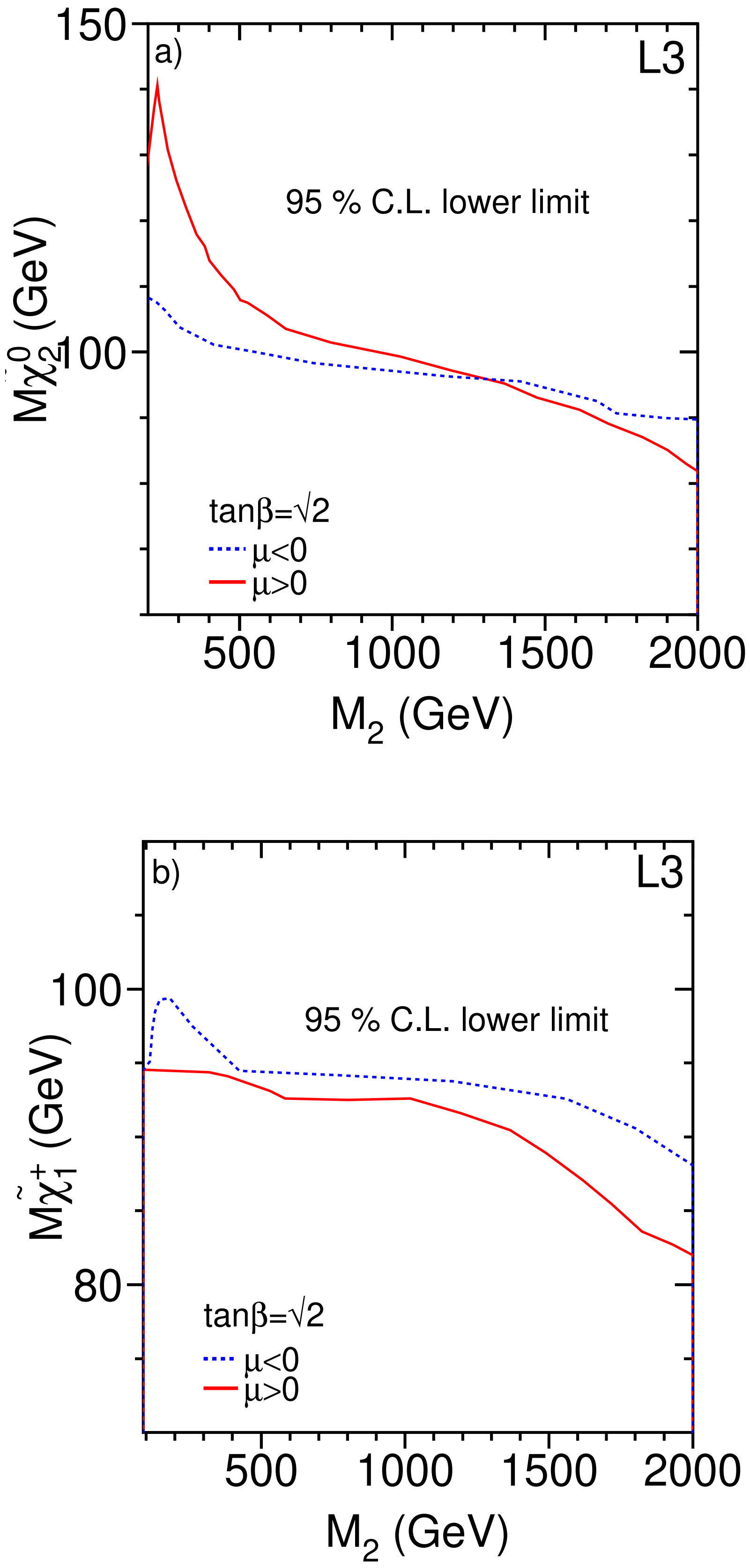

Figure 4: Lower mass limits as a function of M_2 for the next-to-lightest neutralino a) and the lightest chargino b). The limits are shown for $\tan\beta = \sqrt{2}$ and for $\mu > 0$ and $\mu < 0$.

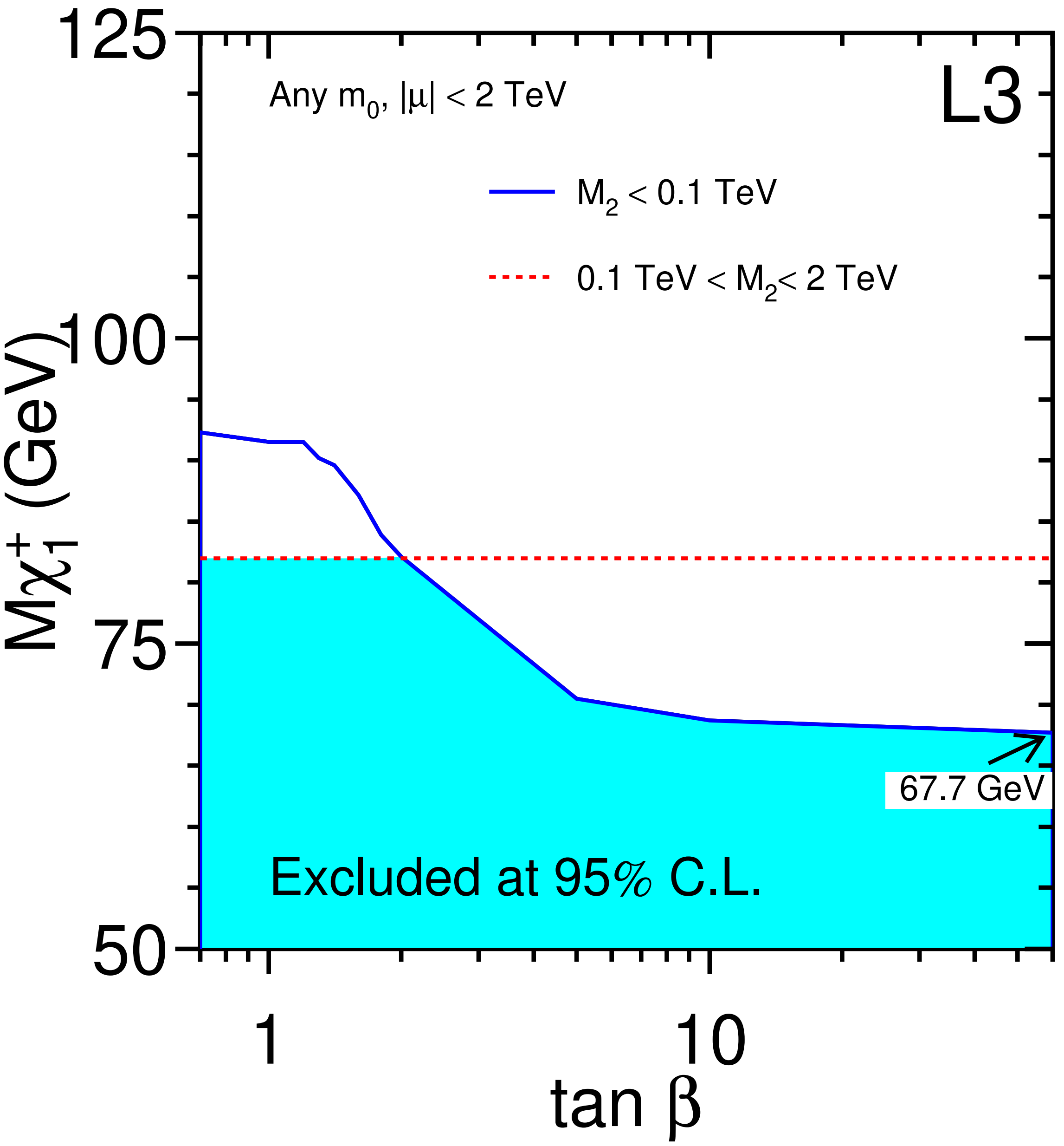

Figure 5: Lower limit on $M_{\tilde{\chi}_1^{\pm}}$ as a function of $\tan\beta$ and for any value of m_0. The solid line (gaugino region) shows the lower limit obtained for light scalar neutrinos (also small M_2 values), which corresponds to the absolute lower limit for large $\tan\beta$ values. The dashed line (higgsino region) shows the lower limit obtained for very small ΔM values. This line corresponds to the absolute lower limit for small $\tan\beta$ values.

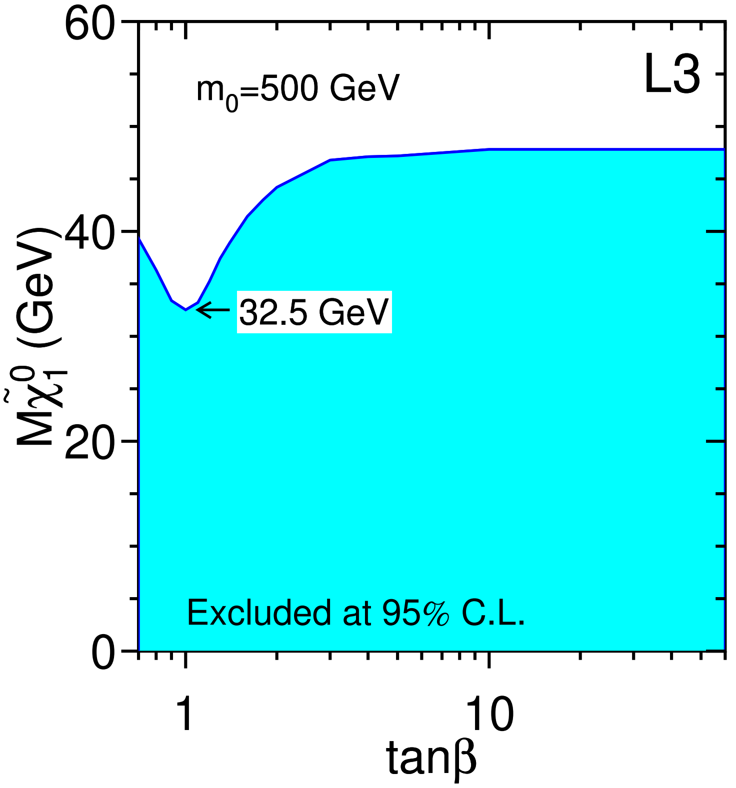

Figure 6: Lower limit on the lightest neutralino mass, $M_{\tilde{\chi}_1^0}$, as a function of $\tan\beta$ for $m_0 =$ 500 GeV, when combining all chargino and neutralino searches.

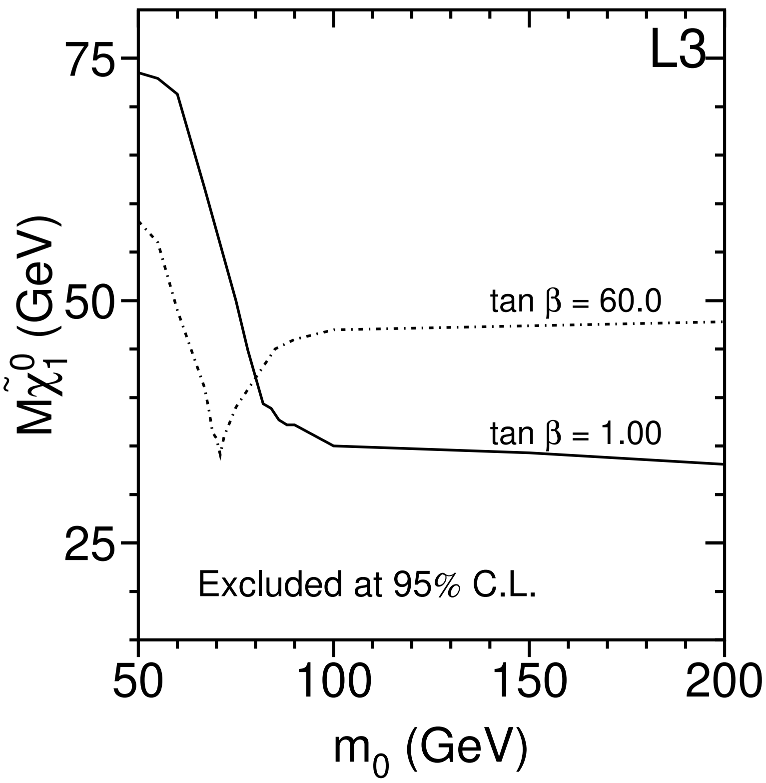

Figure 7: Lower limit on the lightest neutralino mass, $M_{\tilde{\chi}_1^0}$, as a function of m_0 for two values of $\tan\beta$. Scalar lepton searches contribute in the low m_0 region. Chargino searches contribute mainly in the high m_0 region. For the low $\tan\beta$ values, the neutralino searches give additional contribution in the intermediate m_0 region.

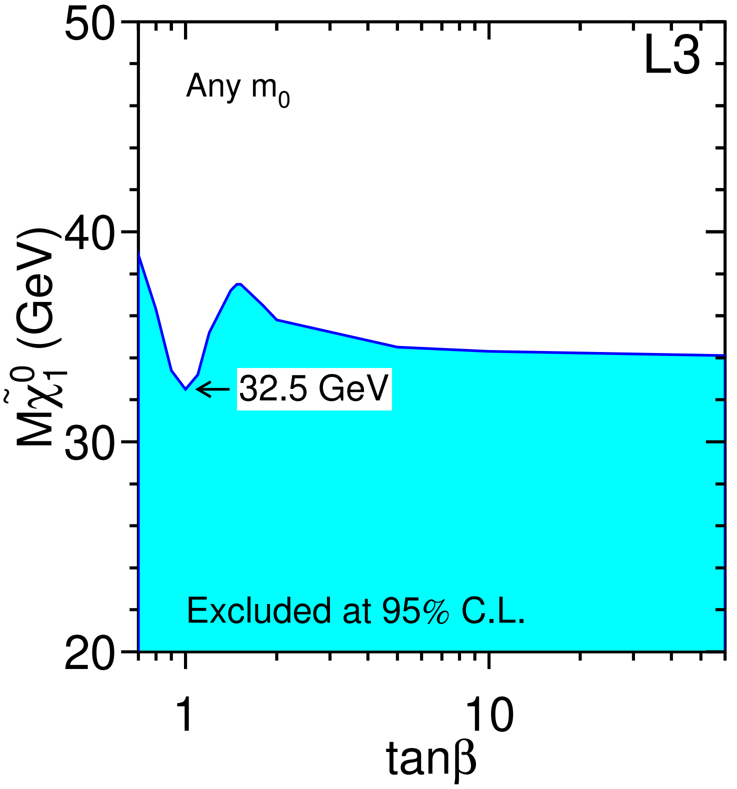

Figure 8: Lower limit on $M_{\tilde{\chi}^0_1}$ as a function of $\tan\beta$ and for any value of m_0, when combining the chargino, neutralino and scalar lepton searches.

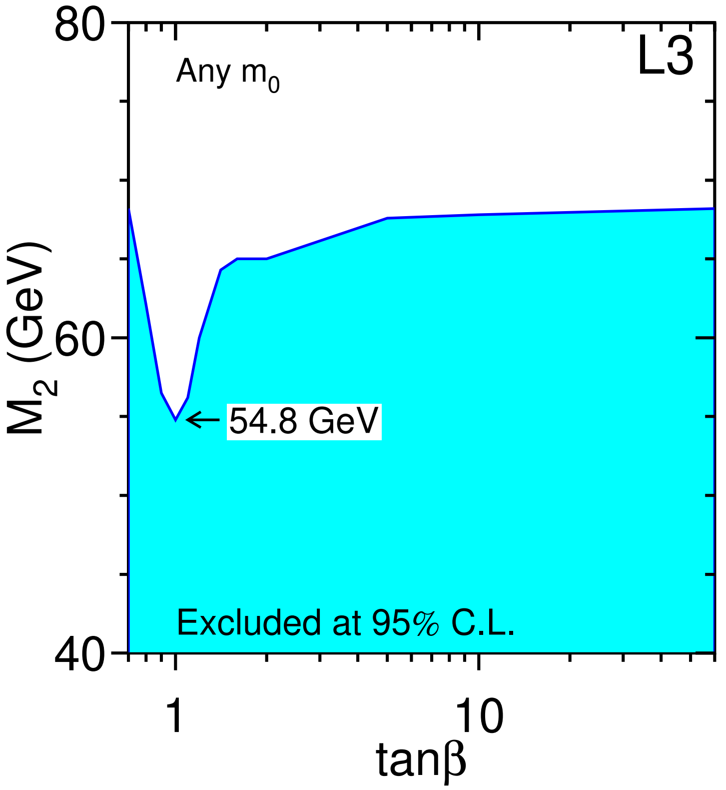

Figure 9: Lower limit on M_2 as a function of $\tan\beta$ and for any value of m_0, when combining the chargino neutralino and scalar lepton searches.